U.S. DEPARTMENT OF THE INTERIOR
U.S. GEOLOGICAL SURVEY

Gravity and Aeromagnetic Models along the Los Angeles Region Seismic Experiment (Line 1), California

By V.E. Langenheim[1]

Open-File Report OF 99-388

1999

U.S. DEPARTMENT OF THE INTERIOR
BRUCE BABBITT, Secretary

U.S. GEOLOGICAL SURVEY
Charles G. Groat, Director

[1] U.S. Geological Survey, MS 989, 345 Middlefield Road, Menlo Park, CA 94025

TABLE OF CONTENTS

Abstract 1
Introduction 1
Acknowledgments 2
Geologic Setting 2
Forward Modeling of Crustal Structure from the Passive Experiment 3
Forward Modeling of Crustal Structure from the Active Experiment 5
Aeromagnetic Data and Modeling 6
Conclusions 8
References 9

TABLES

Table 1. Average Densities from McCaffree Pellerin and Christensen (1998) 12

FIGURES

Figure 1. Shaded-relief topographic map 13
Figure 2. Bouguer gravity map 14
Figure 3. Gravity models of passive experiment 15
Figure 4. Gravity models of active experiment 18
Figure 5. Aeromagnetic map 20
Figure 6. Aeromagnetic models 21

ABSTRACT

The Los Angeles Regional Seismic Experiment (LARSE) was initiated to study the crustal structure and mechanical properties of faults in the Los Angeles region. Colocated with high-resolution seismic-refraction and reflection data are detailed gravity measurements and high-resolution aeromagnetic surveys. Gravity data were modeled to test whether there is a crustal root beneath the San Gabriel Mountains as suggested by analysis of the teleseismic data from the passive phase of the experiment. The detailed gravity data were also modeled using the results of the seismic-refraction data. The gravity modeling indicates that a crustal root is permissible, but requires an offsetting high-density body such as a high-density mantle anomaly. Regardless of whether there is a crustal root, the gravity modeling indicates a substantial density contrast in the upper and middle crust across the San Andreas fault and both gravity and aeromagnetic data indicate a vertical San Andreas fault. The shallow, low-velocity zone centered over the San Andreas fault that apparently dips to the southwest beneath the San Gabriel Mountains may not reflect the actual dip of the San Andreas fault, but fracturing caused by multiple strands of the San Andreas fault zone.

INTRODUCTION

The Los Angeles Regional Seismic Experiment (LARSE) began in 1993 along a profile from Seal Beach to the Mojave Desert (Fig. 1), crossing the Los Angeles basin, San Gabriel Valley basin, and the San Gabriel Mountains, to help characterize the crustal structure at seismogenic depths. The initial phase of the seismic experiment was passive (Kohler and others, 1996), followed by active experiments in 1994 (Fuis and others, 1996). An explosion survey along Line 1 was coincident with the passive profile. Kohler and Davis (1997) model the relative teleseismic travel-time residual patterns from the passive experiment in terms of laterally-varying crustal thickness and a mantle high-velocity anomaly. They indicate a 12-km increase in crustal thickness under the San Gabriel Mountains. These results do not agree with previous regional seismic studies that indicate little or no crustal root beneath the San Gabriel Mountains (Kanamori and Hadley, 1975; Hearn and Clayton, 1986). Furthermore, Bouguer gravity data do not indicate a significant crustal root beneath the San Gabriel Mountains (Fig. 2); Sheffels and McNutt (1986) suggested that the lack of correlation of Bouguer gravity with topography indicates the absence of a classic "Airy root" beneath the mountain range and that the topography of the range is supported by a rigid lithosphere. I present here forward 2-dimensional models of detailed gravity data collected along Line 1 (Langenheim and Jachens, 1996) to determine the relative contributions of crustal and mantle structure to the observed Bouguer gravity anomalies. Regardless of whether the San Gabriel Mountains are supported by a crustal root, density variations in the upper and middle crust are necessary to match the observed gravity data across the San Andreas fault (SAF). I create a gravity model based on the crustal velocity structure of Fuis and others (1996) and show where the velocity-density structure needs to be modified to fit the observed gravity anomalies. I also present magnetic models along the LARSE 1 line to constrain the dip of the SAF.

ACKNOWLEDGMENTS

I thank Gary Fuis and Robert Jachens (both at the U.S. Geological Survey, Menlo Park, CA) for their thoughtful and helpful reviews.

GEOLOGIC SETTING

The LARSE transect crosses several geologic provinces, from the Los Angeles basin across the San Gabriel Mountains to the Mojave Desert (Fig. 1). This region has experienced a complex Tertiary history including subduction, strike-slip faulting, extension, and large-scale rotation (Atwater, 1970; Ehlig, 1975; Crowell, 1976; Crouch and Suppe, 1993; Wright, 1991; Powell, 1993; Luyendyk and Hornafius, 1987).

The San Gabriel Mountains are part of the east-trending Transverse Ranges and lie oblique to the predominant northwest structural grain of California. Their high relief developed in response to north-south compression during the past 2 to 3 million years (Crowell, 1976). In addition, paleomagnetic studies indicate that the rocks of the Transverse Ranges (west of the San Gabriel Mountains) rotated clockwise, beginning in the middle Miocene (Luyendyk and Hornafius, 1987).

The basement rocks of the San Gabriel Mountains are highly varied and consist in part of a suite of Precambrian gneisses, amphibolites, and anorthosites. These rocks are intruded by late Mesozoic granitic rocks and, locally, by the Permo-Triassic Mt. Lowe granodiorite (Ehlig, 1975). This package of rocks forms the upper plate of the Vincent thrust (Fig. 1). The lower plate consists of the Pelona schist, which is greenschist to amphibolite facies and derived from late Mesozoic graywacke, siltstone, shale, and basic volcanic rocks. Matti and Morton (1993) refer to the upper and lower plates of the Vincent thrust fault as the basement rocks of the San Gabriel terrane. These basement rocks are exposed between the San Gabriel and San Andreas faults and correlation of these basement rocks with similar rocks in the Orocopia and Chocolate Mountains 300 km to the southeast permits an estimate of large-scale right-lateral displacement for the southern SAF (Ehlig, 1975).

The Mojave block is a relatively featureless, high-standing (approximately 700 m above sea level) plateau of low relief that is separated into internally drained valleys and gentle mountains. The region is underlain by a pre-Tertiary basement complex consisting largely of Mesozoic plutonic rocks and pendants of metasedimentary and metavolcanic rocks. Near the SAF, the plutonic rocks intrude Proterozoic prebatholithic orthogneiss and metasedimentary rocks that are comparable with rocks of the Cordilleran miogeocline (Stewart and Poole, 1975). The composition of the intrusive rocks ranges from nearly ultramafic to highly silicic, but most exposed plutonic rocks are quartz monzonite or granite in composition (Dibblee, 1981).

The widespread distribution of correlatives of the Pelona schist on the north side of the SAF has led to speculation that Pelona schist-like rocks underlie much of the Mojave and Colorado deserts (Ehlig, 1968; Haxel and Dillon, 1979). Seismic-reflection studies of the western Mojave Desert indeed suggest the subsurface continuation of the Rand schist (a possible correlative of the Pelona schist) over an area of many tens of kilometers (Cheadle and others, 1986). However, a recent interpretation of the LARSE 1 seismic-refraction data (Lutter and others, in press) implies that Pelona schist-like rocks are absent and drilling at Cajon Pass (Fig. 1) found no evidence of the Pelona schist there (Silver and James, 1988).

The San Andreas fault is the major structural element in the San Gabriel-Mojave region. Although the main trace of the fault is thin (< 50 m in width; Dibblee, 1982), Barrows and others (1987) recognize five discrete strands of the SAF (comprising a zone 2-3 km wide), including the Punchbowl fault, in the San Gabriel Mountains region. Their mapping shows that the main San Andreas strand truncates the other four faults on their northwest and southeast ends. These strands evolved sequentially over the past 5 Ma, with the main trace of the SAF originating in middle Pleistocene time. Furthermore, Barrows and others (1987) found evidence of sequential northward shift in the focus of lateral displacement from the Punchbowl fault to today's SAF. Older branches of the SAF system include the San Gabriel fault, about 20 km south of SAF, and the Fenner-San Francisquito-Clemens Well fault, which is offset by branches of the modern SAF (Powell, 1993)

FORWARD MODELING OF CRUSTAL STRUCTURE FROM THE PASSIVE EXPERIMENT

Gravity data were collected along the LARSE 1 profile (Langenheim and Jachens, 1996). The gravity data were modeled in stages. The first part of the gravity modeling is to test whether a crustal root beneath the San Gabriel Mountains is permissible. Densities were assigned to the various bodies in the cross-section of Kohler and Davis (1997). I used the velocity structure of Hadley and Kanamori (1977) to determine the depth of the upper crust-lower crust transition. I assumed that the upper crustal density was 2670 kg/m^3 and the upper crust was 15 km thick. I then assigned a density, ρ, of 2880 kg/m^3 to the lower crust, using a velocity, V_p, of 6.5 km/s and the following relationship of Christensen and Mooney (1995) for rocks at 10 km depth:

$$\rho = 540.6 + 360.1 V_p \qquad (1)$$

A single density contrast of -250 kg/m^3 was assumed for the sedimentary deposits of the Los Angeles basin. I used a velocity of 7.8 km/s for "normal" mantle and 8.3 km/s for the "anomalous", high-velocity mantle beneath the Transverse Ranges (Hadley and Kanamori, 1977). The corresponding densities of 3306 and 3421 kg/m^3 were based on the relationship of Christensen and Mooney (1995) for rocks at 40 km depth:

$$\rho = 5212 - (14863/V_p) \qquad (2)$$

The first model (Fig. 3a) shows what Bouguer gravity anomalies would result if (1) there were no lateral crustal or mantle density variations in the layers shown and (2) a crustal root existed such as modeled by Kohler and Davis (1997). The greatest mismatch occurs over the Mojave Desert if I assume the base levels are correct for the Los Angeles portion of the profile. Adding a high-density body based on the velocity of 8.3 km/s, using the geometry of Humphreys and others (1984), reduces some of the mismatch over the Mojave Desert, but increases it to the south (Fig. 3b). The steepness of the complete Bouguer gravity gradient between the San Gabriel Mountains and Mojave Desert and its correlation to the trace of the SAF over a distance of greater than 100 km (Fig. 2) require crustal sources.

The need for crustal sources to fit the observed gravity data is supported by density and velocity measurements that indicate at least part of the apparent change in basement gravity could be caused by upper crustal rocks. McCaffree Pellerin and Christensen (1998) found that the Mendenhall gneiss and the San Gabriel anorthosite complex have seismic velocities of 6.5 and 6.4 km/s, significantly higher than the average velocity of Mojave granitic rocks of 5.7 km/s. If a reasonable density contrast of 100 kg/m^3 is used for the rocks of the San Gabriel Mountains and the Mojave Desert, the calculated anomaly is still too high over the Transverse Ranges (curve C in Fig. 3c) assuming an anomalous mantle density of 3421 kg/m^3. A more reasonable density for the anomalous mantle is based on the tomographic results of Humphreys and others (1984), where they found mantle 2 - 3% faster under the Transverse Ranges region than elsewhere (white contours on Fig. 2). This 3% faster mantle corresponds to a 500°C decrease and 1% increase in density (Humphreys and Hager, 1990). Curve D on Figure 3c shows that the combination of the mantle anomaly, based on a smaller density contrast, and crustal root does not fit the gravity field over the Mojave Desert. Only when crustal density variations are included in the model do the base levels fit for the Los Angeles Basin, the San Gabriel Mountains, and the Mojave Desert (curve E on Figure 3c).

Could slower mantle under the Mojave Desert eliminate the need for crustal sources? Humphreys and others (1984) do show slower velocities in the upper 50 km north of the Transverse Ranges; the mantle velocity anomalies, however, trend nearly east-west and therefore do not parallel the SAF as does the Bouguer gravity gradient (Fig. 2). Furthermore, Kohler (1999) shows that inclusion of lower mantle velocities beneath the Mojave Desert still cannot match the observed modeled Bouguer gravity using a constant density for the most of the crust (Fig. 3d). Her calculated curve matches the observed data only over the San Gabriel Valley. The misfit over the San Gabriel Mountains and Mojave Desert ranges from 10 to 40 mGal and reinforces results presented here for crustal density variations in order to fit the observed gravity data.

One can fit the gravity data with a crustal root without the mantle anomaly; however, the Mojave block would require a density contrast of 150 kg/m^3 extending to 15 km at the northern end of the

LARSE transect, decreasing in thickness towards the San Andreas fault in correlation with the increase in the thickness of the crustal root. This geometry seems unlikely over the entire Mojave region as does the presence of densities of 2560 kg/m^3 at 15 km depth.

FORWARD MODELING OF CRUSTAL STRUCTURE FROM THE ACTIVE EXPERIMENT

The second stage in the gravity modeling is to convert the velocity model presented in Fuis and others (1996) into a density model using the velocity-density relationships of Gardner and others (1974) and Christensen and Mooney (1995). For velocities less than 5.0 km/s, the relationship of Gardner and others (1974) developed for sedimentary rocks (where ρ is density in g/cm^3 and v is velocity in ft/s) was used:

$$\rho = 0.23v^{0.25} \qquad (3)$$

For velocities greater than 5.5 km/s, equation (1) was used. Curve A (Fig. 4a) shows the calculated gravity anomaly with the crustal root of Kohler and Davis (1997)--accounting for the crustal density variations based on the LARSE seismic-refraction data still is unable to eliminate the large mismatch over the San Gabriel Mountains. Curve B shows that adding the high-velocity mantle beneath the San Gabriel Mountains does not significantly improve the fit over the San Gabriel Mountains (Fig. 4a). The package of rocks with velocities between 5 and 6 km/s centered over km 90 contributes to the calculated gravity low north of the San Gabriel fault, already caused by the crustal root. Even assuming that the high-velocity mantle anomaly corresponds to a density of 3421 kg/m^3 does not reduce the mismatch and even worsens the calculated-observed fit on the southern end of the profile.

The following describes how the velocity-density model can be modified to fit the observed gravity data. The discrepancy between the calculated values and the observed gravity data on the southern end of the profile (Fig. 4a; where velocities would be more poorly constrained) can be improved by making the basement shallower. This is supported by well data that penetrated basement rocks along the Newport-Inglewood fault zone (Yerkes and others, 1965) at depths of 3 to 4 km. The mismatch in the region between the Whittier and Sierra Madre faults is eliminated by slightly reducing the density of the basement rocks in this area. Part of the discrepancy in the calculated and observed values in Figure 4a near the San Andreas fault is resolved by recognizing that extensive fracturing most likely causes the low velocities observed in the upper 1-2 km and would not affect the densities as severely. For example, a study of granitic rocks in a well about 1 km from the San Andreas fault in the Gabilan Range (450 km to the northwest) found that saturated macrocracks produced 3-7% reduction in the rock density, but a 30-50% reduction of *in situ* seismic velocities (Stierman and Kovach, 1979).

The rest of the discrepancy between the velocity and density models is eliminated by extending a constant density contrast along a vertical San Andreas fault to depths of 10 km. I find that higher-density rocks are needed in the San Gabriel Mountains--higher than would be predicted from the velocities measured on the LARSE 1 transect and the velocity-density relationship of Christensen and Mooney (1995) for crystalline rocks, even in the case where there is no crustal root (Fig. 4b). The depth extent of this density contrast is not well constrained; reducing the density contrast and increasing the depth extent can produce essentially the same curve. For example, increasing the depth extent to 20 km from 10 km reduces by half the density contrast to produce the same calculated curve. However, surface density measurements suggest that a depth extent of 10 km may be more reasonable. The average density of crystalline rocks in the San Gabriel terrane (based on 102 samples in the Geophysical Unit Menlo Park physical property database, U.S. Geological Survey) is 2730 kg/m^3. The average density of Mojave pre-Cenozoic rocks is 2670 kg/m^3 (based on 111 samples). Most of the exposed rocks in the Mojave terrane are intrusive rocks; density measurements of the Mojave intrusive rocks indicate an average of 2650 kg/m^3 (based on 68 samples). This average is substantially higher than that reported in McCaffree Pellerin and Christensen (1998; Table 1).

If the depth extent of this density contrast is on the order of 10 km, it should be reflected in the rock compositions at 3 - 6 km depth proposed by McCaffree Pellerin and Christensen (1998). They compared seismic velocities measured on samples in the laboratory with increasing pressure with velocity gradients measured on the LARSE 1 profile. Based on this comparison, they suggest that the upper crust of the Mojave terrane consists mostly of Mojave gneisses, whereas the crust beneath the San Gabriel terrane consists of anorthosite and Mendenhall gneisses. Their average density of Mojave gneisses is 2830 kg/m^3; whereas the combined average density of the anorthosite and Mendenhall gneiss is 2800 kg/m^3. The resulting density contrast would be opposite that required to produce the observed gravity data. Incorporating lower-density (2720 kg/m^3; Table 1) Pelona schist (which form the lower plate of the Vincent thrust and must underlie the San Gabriel Mountains segment of the LARSE 1 transect) exacerbates the problem. Only if the San Gabriel crust is substantially composed of Mendenhall gneiss could these rocks produce the required density contrast with crust composed of Mojave gneisses. Their analysis is based on averages of only a few samples that have considerable range in both velocity and density (Table 1).

AEROMAGNETIC DATA AND MODELING

My best-fitting gravity models (Fig. 3c and Fig. 4b) indicate a vertical San Andreas fault with or without a crustal root. I also examined aeromagnetic data along the LARSE 1 line to determine if these data also indicate a vertical San Andreas fault. High-resolution aeromagnetic data were collected over the LARSE 1 region in 1995 (U.S. Geological Survey, 1996) and added to existing high-resolution data collected over the Peninsular Ranges. Most of the new data were flown along N-S trending flightlines spaced 800 m apart with an average terrain clearance of 550 m.

The LARSE 1 transect crosses the San Andreas fault obliquely. I modeled along a single straight-line profile that is normal to the trend of the San Andreas fault (Fig. 5). A narrow (less than 10 km) magnetic high coincides with the trace of the SAF for at least 100 km. The lack of a corresponding aeromagnetic low to the northeast indicates that the Mojave terrane is underlain by magnetic rocks. The magnetic data show elevated values over a broad region of the Mojave Desert (east of a line from about latitude 34°30' north, longitude 118°west to about latitude 34°55' north, longitude 117°40'; Fig. 5). Another feature in the aeromagnetic data that the transect crosses is a broad aeromagnetic high over the Los Angeles basin. This high appears to be a continuation of the more intense aeromagnetic high over the San Joaquin Hills to the southeast (Fig. 5). The transect obliquely crosses an aeromagnetic high bounded in part by the San Jose fault (Fig. 1).

The gridded data along the straight-line transect were upward continued 500 m to eliminate many of the short-wavelength features. The models of the aeromagnetic data attempt to constrain the geometry of the regional features along the profile. I do not attempt to fit every anomaly, but concentrate on those that might affect the modeling of the San Andreas aeromagnetic anomaly. Thus the models fit the long-wavelength Los Angeles basin anomaly and the anomaly bounded by the San Jose fault. The geometry of the San Jose anomaly is poorly constrained as the transect crosses the anomaly at a highly oblique angle; the geometry of the Los Angeles basin anomaly is consistent with previous modeling indicating a thick body with a moderately northeast-dipping southern boundary (Langenheim and Jachens, 1993). The geometry of these two bodies is approximately the same in the two sets of models presented (Fig. 6). The models indicate that the dip of the SAF is sensitive to the thickness of the magnetic block beneath the Mojave Desert.

Fig. 6a assumes that the magnetic block beneath the Mojave Desert is 8 km thick. The calculated anomaly produced by a vertical southern edge of the Mojave magnetic block matches fairly well the sharp gradient and amplitude of the observed aeromagnetic anomaly. Decreasing the dip on the southern margin by even 10° to the northeast causes the calculated anomaly to deviate from the observed data, especially at the base of the sharp gradient. A slightly better fit to the observed data results if the southern margin dips slightly to the southwest. If the body is only 3 km thick, the SAF must dip moderately in order for the calculated values to match the observed data (Fig. 6b). The models in Fig. 6b, however, present a geologically unseemly geometry over a very large area (100 km by 80 km).

The velocity model of the LARSE 1 profile (Fuis and others, 1996) indicates a low-velocity zone that dips to the southwest beneath the San Gabriel terrane; however, Fuis and others (1998) estimate a San Andreas fault that dips slightly to the northeast, based on truncated reflections at approximately 20 km depth (Ryberg and Fuis, 1998). Seismicity (taken from the southern

California seismic network and based on a one-dimensional velocity structure) does suggest a slight southwest dip to the San Andreas fault. However, observed seismicity does not coincide exactly with the edge of the modeled body, but is displaced 1-2 km to the northeast. The locations of the earthquakes may suffer from a systematic error caused by the strong velocity and density variations across the San Andreas fault or perhaps they are occurring on the southeast extension of the Little Rock strand of the San Andreas fault in this area. The low velocities centered over the San Andreas fault dipping to the southwest may reflect fracturing on these multiple strands of the fault.

Another consequence of the magnetic model is the extent of the Pelona schist beneath the Mojave Desert in this area. The Pelona schist in the San Gabriel Mountains does not produce significant aeromagnetic anomalies. The favored magnetic model indicates magnetic material extending to depths of 8 km. This suggests that Pelona schist, if present in the subsurface of the Mojave Desert in the LARSE 1 region, is present at depths greater than 8 km. This conclusion is supported by a recent seismic-refraction interpretation by Lutter and others (in press) of the LARSE 1 data. If this is the case, this casts doubt on the conclusions of Magistrale and Zhou (1996) that the shallowing of seismicity in this region is caused by the Pelona schist.

CONCLUSIONS

The application of 2-dimensional gravity modeling of the LARSE 1 transect indicates that a crustal root as proposed by Kohler and Davis (1997) is permissible, but either requires unlikely density contrasts in the crust or higher-density mantle beneath the San Gabriel Mountains. The fit is easier to obtain if the observed velocity increase from tomographic work produces one-third the equivalent density increase. The gravity modeling also shows that a crustal root is not necessary to match the observed data. Regardless of whether there is a crustal root, a significant gravity gradient exists across the San Andreas fault. This change in gravity cannot be explained by the crustal root or variations in mantle density because the gradient coincides with the San Andreas and San Jacinto faults (Fig. 2). The Transverse Ranges and its proposed crustal root and the high-velocity mantle cut across the gradient at a high angle (Fig. 2). The source of the gravity gradient is, therefore, in the crust, not the mantle. Models of the gravity and aeromagnetic data indicate that the San Andreas fault is near-vertical to depths of 10 km. The low velocity zone of Fuis and others (1996) most likely reflects fracturing associated with multiple strands of the San Andreas fault in this region.

REFERENCES

Atwater, T., 1970, Implications of plate tectonics for the Cenozoic tectonic evolution of western North America: Geological Society of America Bulletin, v. 81, p. 3513-3535.

Barrows, A.G., Kahle, J.E., and Beeby, D.J., 1987, Earthquake hazards and tectonic history of the San Andreas fault zone, Los Angeles County, California *in* Hester, R.L., and Hallinger, D.E., eds., San Andreas fault--Cajon Pass to Palmdale: Pacific Section, American Associationof Petroleum Geologists Volume and Guidebook 59, p. 1-92.

Cheadle, M.J., Czuchra, B.L., and Byrne, T., Ando, C.J., Oliver, J.E., Brown, L.D., Malin, P.E., and Phinney, R.A., 1986, The deep crustal structure of the Mojave Desert, California, from COCORP seismic reflection data: Tectonics, v. 5, p. 293-320.

Christensen, N.I., and Mooney, W.D., 1995, Seismic velocity structure and composition of the continental crust: A global view: Journal of Geophysical Research, v. 100, no. B7, p.9761-88.

Crouch, J.K., and Suppe, John, 1993, Late Cenozoic tectonic evolution of the Los Angeles basin and inner California borderland: A model for core complex-like crustal extension: Geological Society of America Bulletin 105, no. 11, p. 1415-1434.

Crowell, J.C., 1976, Implications of crustal stretching and shortening of coastal Ventura basin, California *in* D.G. Howell, ed., Aspects of the geologic history of the California continental borderland: Pacific Section, AAPG, Misc. Publ. 24, p. 365-382.

Dibblee, T.W., Jr., 1981, Regional structure of the Mojave Desert: U.S. Geological Survey Open-File Report 81-503, p. 26-28.

Dibblee, T.W., Jr., 1982, Tectonics of the San Gabriel Mountains, southern California *in* Fife, D.L., Minch, J.A., (eds.), Geology and Mineral Wealth of the California Transverse Ranges: South Coast Geological Society Guidebook No. 16, p. 148-169

Ehlig, P.L., 1968, Causes of distribution of Pelona, Rand, and Orocopia Schists along the San Andreas and Garlock faults, in Dickinson, W.R., and Grantz, A., eds., Proceedings of Conference on Geologic Problems of San Andreas Fault Systems: Stanford, California, Stanford University Publications in the Geological Sciences, V. 11, p. 294-306.

Ehlig, P.L., 1975, Basement rocks on the San Gabriel Mountains, south of the San Andreas fault: California Division of Mines and Geology Bulletin 118, p. 177-187.

Fuis, G.S., Lutter, W.J., Murphy, J.M., Ryberg, T., Thurber, C.H., and Shaw, J.H., Imaging faults in the Los Angeles region, southern California, using seismic data from the Los Angeles Region Seismic Experiment (LARSE): EOS Transactions American Geophysical Union, v. 79, p. F591.

Fuis, G.S., Okaya, D.A., Clayton, R.W., Lutter, W.J., Ryberg, T., Brocher, T.M., Henyey, T.M., Benthien, M.L., Davis, P.M., Mori, J., Catchings, R.D., ten Brink, U.S., Kohler, M.D., Klitgord, K., and Bohannon, R.G., 1996, Images of crust beneath Southern California will aid study of earthquakes and their effects: Eos, Trans., Am. Geophys. Union, v. 77, p. 173-176.

Gardner, G.H., Gardner, L.W., and Gregory, A.R., 1974, Formation velocity and density: the diagnostic basis for stratigraphic traps: Geophysics, v. 39, p. 770-780.

Hadley, D., and Kanamori, H., 1977, Seismic structure of the Transverse Ranges, California: Geological Society of America Bulletin, v. 88, p.1469-1478.

Haxel, G.B., and J.T. Dillon, The Pelona-Orocopia schist and Vincent-Chocolate Mountain thrust system, southern California, in Mesozoic Paleogeography of the Western United States, edited by D.G. Howell and K.A McDougall, Los Angeles, Society of Economic Paleontologists and Mineralogists, Pacific Section, Pacific Coast Paleogeography Symposium 2, 453-469, 1978.

Hearn, T.M., and Clayton, R.W., 1986, Lateral velocity variations in southern California. II. Results from the lower crust from Pn waves: Bulletin of the Seismological Society of America, v. 76, p. 511-520.

Humphreys, E., Clayton, R., and Hager, B.H., 1984, A tomographic image of mantle structure beneath southern California: Geophysical Research Letters, v. 11, no. 7, p. 625-27.

Humphreys, E., and Hager, B.H., 1990, A kinematic model for the late Cenozoic development of southern California crust and upper mantle: Journal of Geophysical Research, v. 95, no. B12, p. 19747-19762.

Kanamori, H., and Hadley, D., 1975, Crustal structure and temporal velocity changes in southern California: Pure and Applied Geophysics, v. 113, p. 257-280.

Kohler, M.D., 1999, Lithospheric deformation beneath the San Gabriel Mountains in the southern California Transverse Ranges: Journal of Geophysical Research, v. 104, no. B7, p. 15,025-15,041.

Kohler, M.D., and Davis, P.M., 1997, Crustal thickness variations in southern California from Los Angeles Region Seismic Experiment passive phase teleseismic travel times: Bulletin of the Seismological Society of America, v. 87, no. 5, p. 1330-1344.

Kohler, M.D., Davis, P.M., Liu, H., Benthien, M., Gao, S., Fuis, G.S., Clayton, R.W., Okaya, D., and Mori, J., 1996, Data report for the 1993 Los Angeles Regional Seismic Experiment (LARSE93), Southern California: a passive study from Seal Beach northeastward through the Mojave Desert: U.S. Geological Survey Open-File Report 96-85.

Langenheim, V.E., and Jachens, R.C., 1996, Gravity data collected along the Los Angeles Regional Seismic Experiment (LARSE) and preliminary model of regional density variations in basement rocks, southern California: U.S. Geological Survey Open-File Report 96-682.

Langenheim, V.E., and Jachens, R.C., 1993, Nature of basement rocks under the Los Angeles basin, southern California, as inferred from aeromagnetic data: GSA Abstracts with Programs, v. 25, p. 66.

Lutter, W.J., Fuis, G.S., Thurber, C.H., and Murphy, J.M., Tomographic images of the upper crust from the Los Angeles basin to the Mojave Desert, California: results from the Los Angeles Region Seismic Experiment: Journal of Geophysical Research (in press).

Luyendyk, B.P., and Hornafius, J.S., 1987, Neogene crustal rotations, fault slip, and basin development in southern California, *in* R.V. Ingersoll and W.G. Ernst, Eds., Cenozoic basin development of coastal California: Englewood Cliffs, New Jersey, Prentice-Hall, Inc., Rubey v. VI, p. 259-283.

Magistrale, H., Zhou, H.-W., 1996, Lithologic control of the depth of earthquakes in southern California: Science, v. 273, p. 639-643.

Matti, J.C., and Morton, D.M., 1993, Paleogeographic evolution of the San Andreas fault in southern California: A reconstruction based on a new cross-fault correlation *in* Powell, R.E., Weldon, R.J., II, and Matti, J.C. (eds.), The San Andreas Fault System: Displacement, Palinspastic Reconstruction, and Geologic Evolution: Geological Society of America Memoir 178, p. 107-159.

McCaffree Pellerin, C.L., and Christensen, N.I., 1998, Interpretation of crustal seismic velocities in the Mojave-San Gabriel region, southern California: Tectonophysics, v. 286, p. 253-271.

Powell, R.E., Balanced palinspastic reconstruction of pre-late Cenozoic paleogeology, southern California: Geologic and kinematic constraints on evolution of the San Andreas fault system, *in* The San Andreas Fault System: Displacement, Palinspastic Reconstruction, and Geologic Evolution, edited by R.E. Powell, R.J. Weldon II, and J.C. Matti, Geological Society America Memoir 178, 1-106, 4 plates, 1993.

Ryberg, T., and Fuis, G.S., 1998, The San Gabriel Mountains bright reflective zone: possible evidence of young mid-crustal thrust faulting in southern California: Tectonophysics, v. 286, p. 31-46.

Sheffels, B., and McNutt, M., 1986, Role of subsurface loads and regional compensation in the isostatic balance of the Transverse Ranges: evidence for intracontinental subduction: Journal of Geophysical Research, v. 91, p. 6419-6431.

Silver, L.T., and James, E.W., 1988, Geologic setting and lithologic column of the Cajon Pass deep drillhole: Geophysical Research Letters, v. 15, p. 941-944.

Stewart, J.H., and Poole, F.G., 1975, Extension of the Cordilleran miogeosynclinal belt to the San Andreas fault, southern California: Geological Society of America Bulletin, v. 86, p. 205-212.

Stierman, D.J., and Kovach, R.L., 1979, An in situ velocity study: the Stone Canyon well: Journal of Geophysical Research, v. 84, no. B2, p. 672-678.

U.S. Geological Survey, 1996, Aeromagnetic map of parts of the Los Angeles, San Bernardino, Bakersfield, Long Beach, and Santa Ana 1° by 2° quadrangles, California: U.S. Geological Survey Open-File Report 96-550, scale 1:250,000.

Wright, T.L., Structural Geology and Tectonic Evolution of the Los Angeles Basin, California, in *Active Margin Basins*, edited by K.T. Biddle. American Association of Petroleum Geologists Memoir 52, 35-134, 1991.

Yerkes, R.F., McCulloh, T.H., Schoelhamer, J.E., and Vedder, J.G., 1965, Geology of the Los Angeles basin, California--an introduction: U.S. Geological Survey Professional Paper 420-A, 57 p.

Table 1. Average densities* from McCaffree Pellerin and Christensen (1998)

Southwest of San Andreas (San Gabriel)	Number	Average Density kg/m^3	Density Range kg/m^3	Velocity Range** km/s
San Gabriel gneiss	7	2805	2655-2936	5.749-6.299
Mendenhall gneiss	2	2879	2694-3064	6.010-6.907
Intrusives	5	2696	2571-2795	5.639-6.325
Anorthosite Complex	3	2727	2666-3089	6.162-6.435
Pelona Schist	7	2719	2648-3030	5.579-6.438
Northeast of San Andreas (Mojave)				
Gneiss	5	2830	2656-2896	5.779-6.639
Intrusives	4	2603	2527-2788	5.285-6.055

*Weighted by their estimated percent volume at surface
** Velocities at 150 Mpa measured in the laboratory.

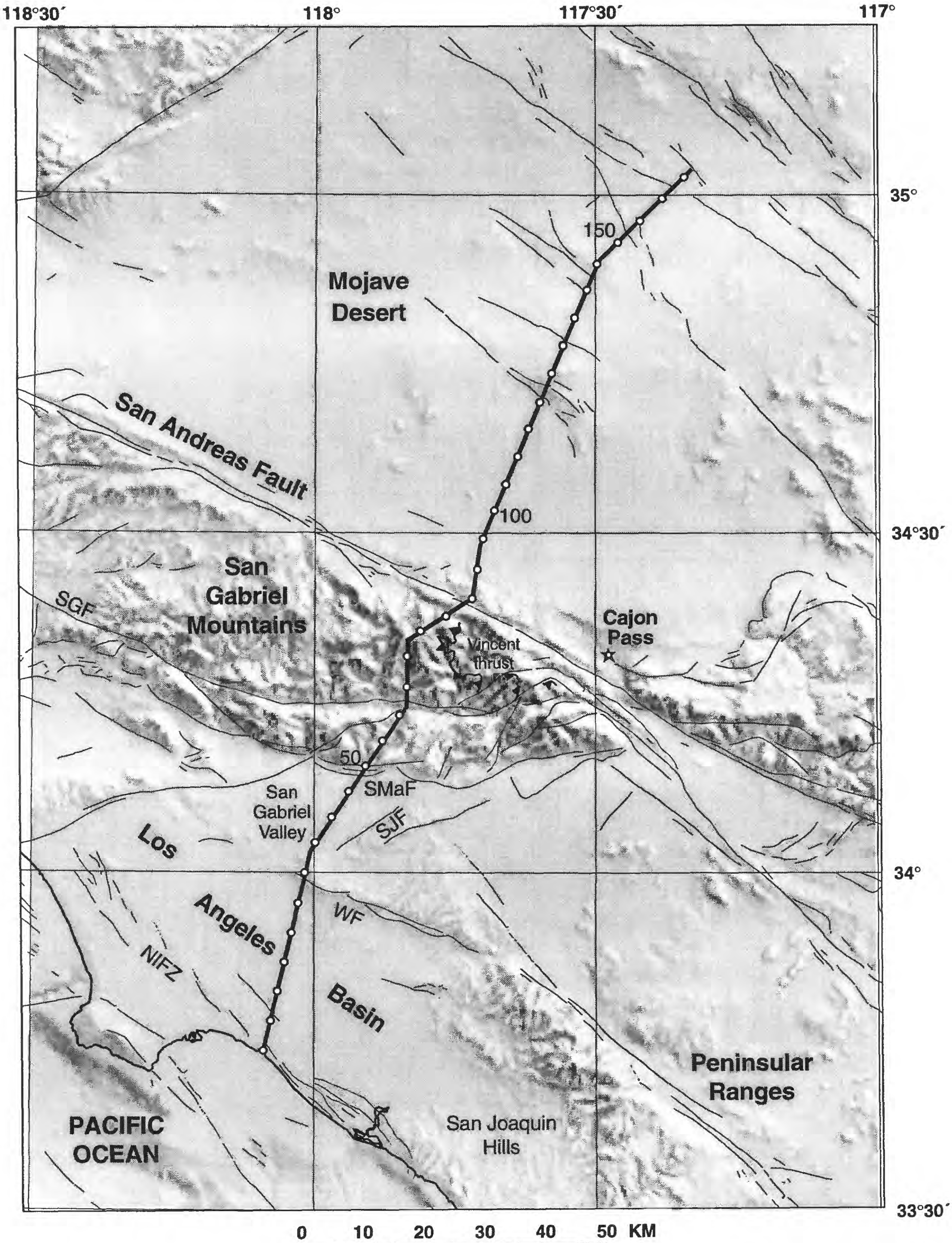

Figure 1. Shaded-relief topographic map of the LARSE 1 transect (heavy black line). White circles mark 5-km increments along the transect. Star marks Cajon Pass well site. NIFZ, Newport-Inglewood fault zone; SGF, San Gabriel fault; SJF, San Jose fault; SMaF, Sierra Madre fault; WF, Whittier fault.

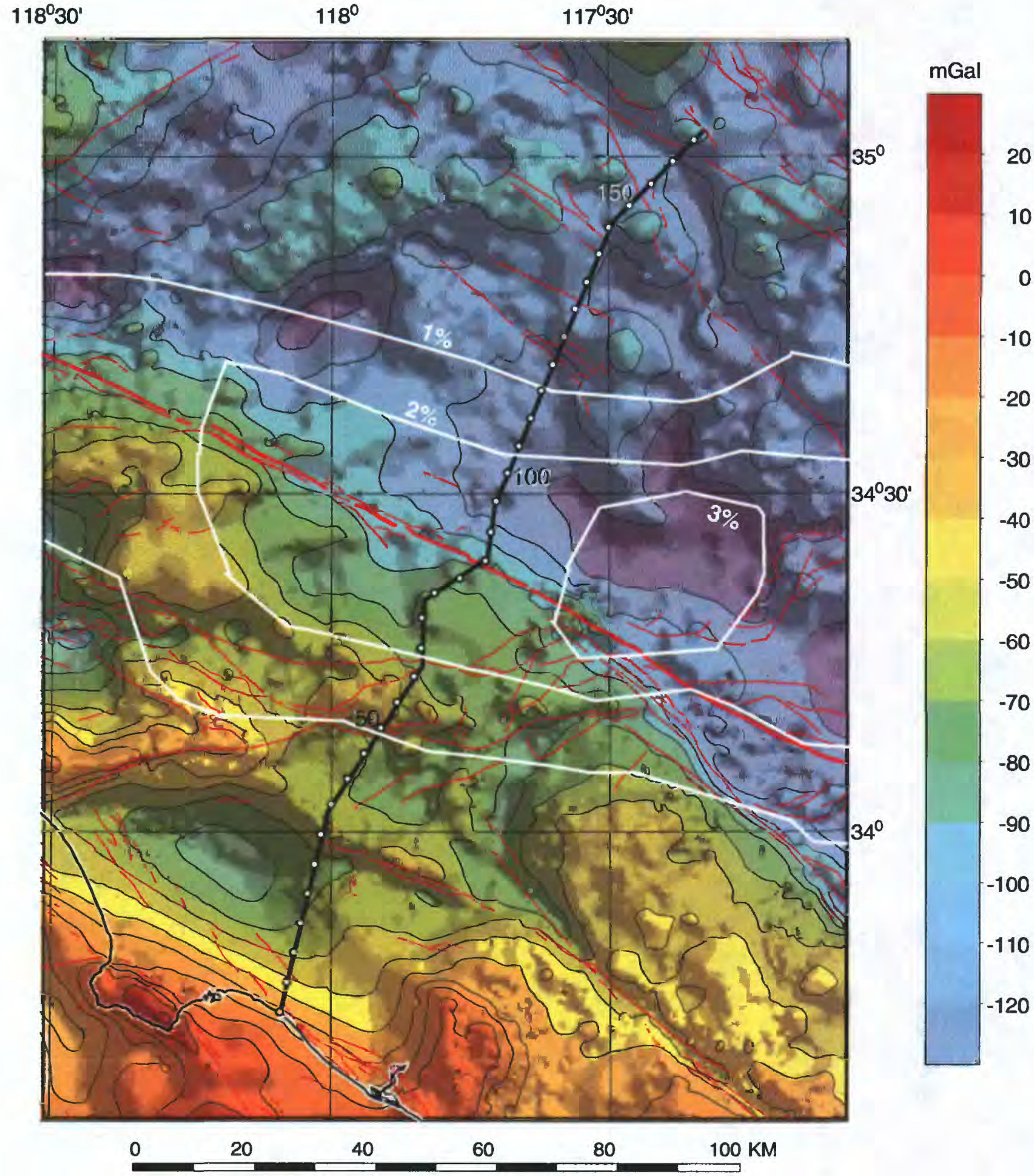

Figure 2. Complete Bouguer gravity anomaly map of LARSE 1 region. Contour interval, 10 mGal. Thick black line is LARSE 1 transect. White circles mark 5 km increments along the LARSE 1 transect. White lines are contours of percent velocity anomaly (Humphreys and others, 1984). Red lines are faults; heavier red line is the San Andreas fault.

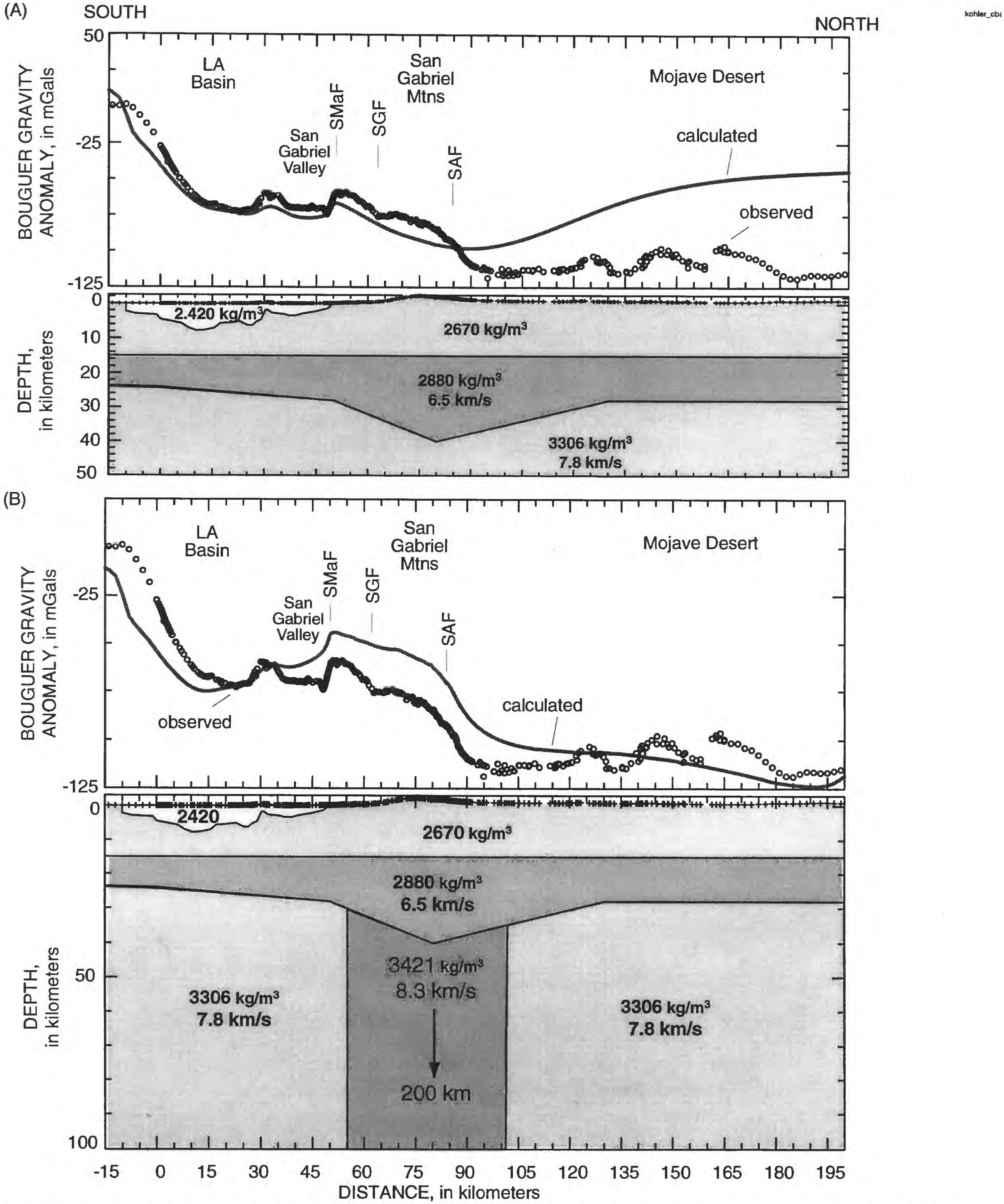

Figure 3. Gravity models of the crustal-mantle interface in Kohler and Davis (1997) along LARSE 1 profile (Figure 1). (A) Model with only a crustal root; (B) crustal root and a body representing the high-velocity anomaly beneath the Transverse Ranges.

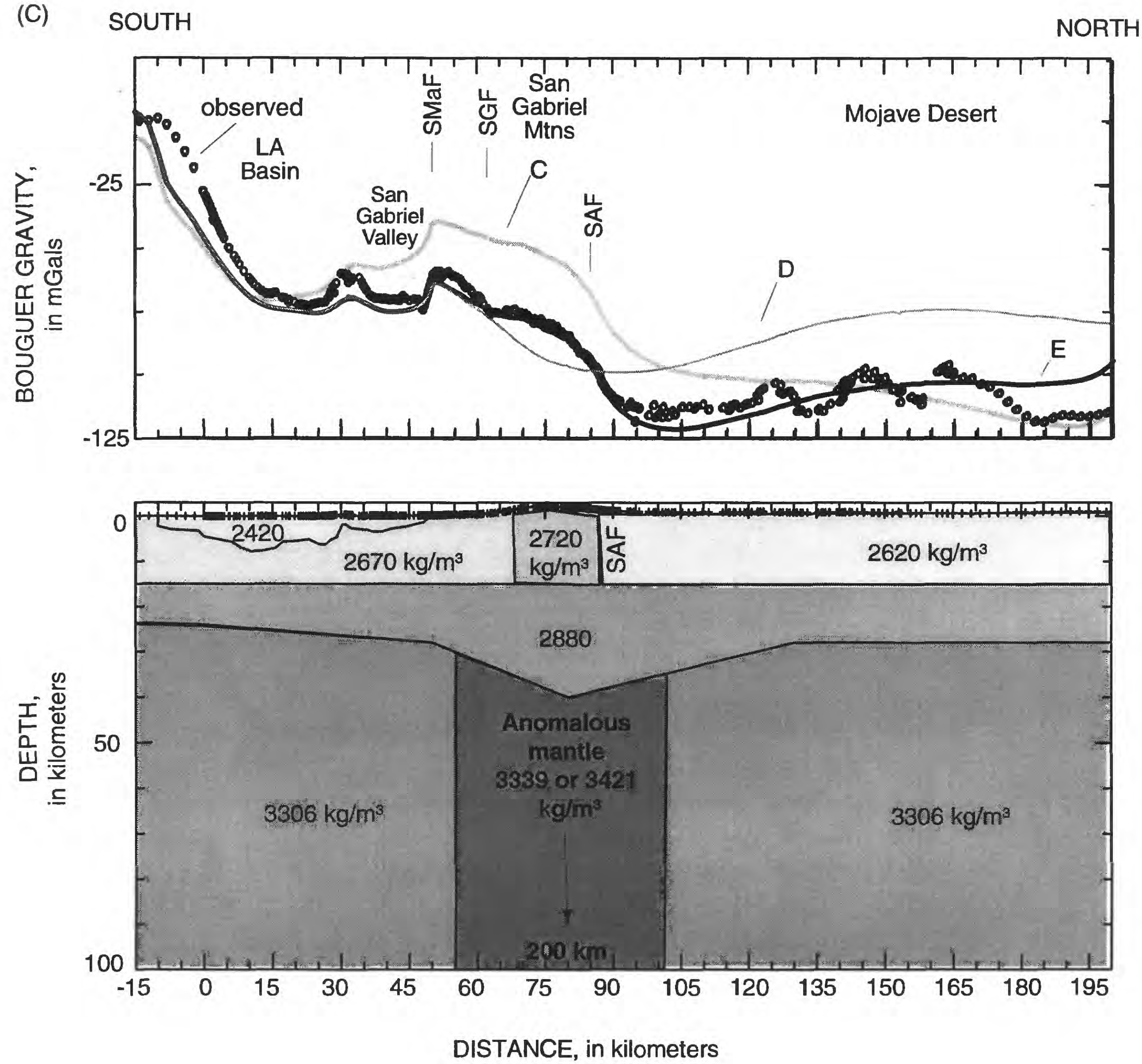

Figure 3C. Gravity model. Curve C is the calculated curve with a density of 3421 kg/m^3 for the anomalous mantle and crustal variations. Curve D is the calculated curve if the anomalous mantle has a density of 3339 kg/m^3, but without any crustal density variations. Curve E, which fits the best, is the calculated curve using crustal density variations and a density of 3339 kg/m^3 for the anomalous mantle. SAF, San Andreas fault.

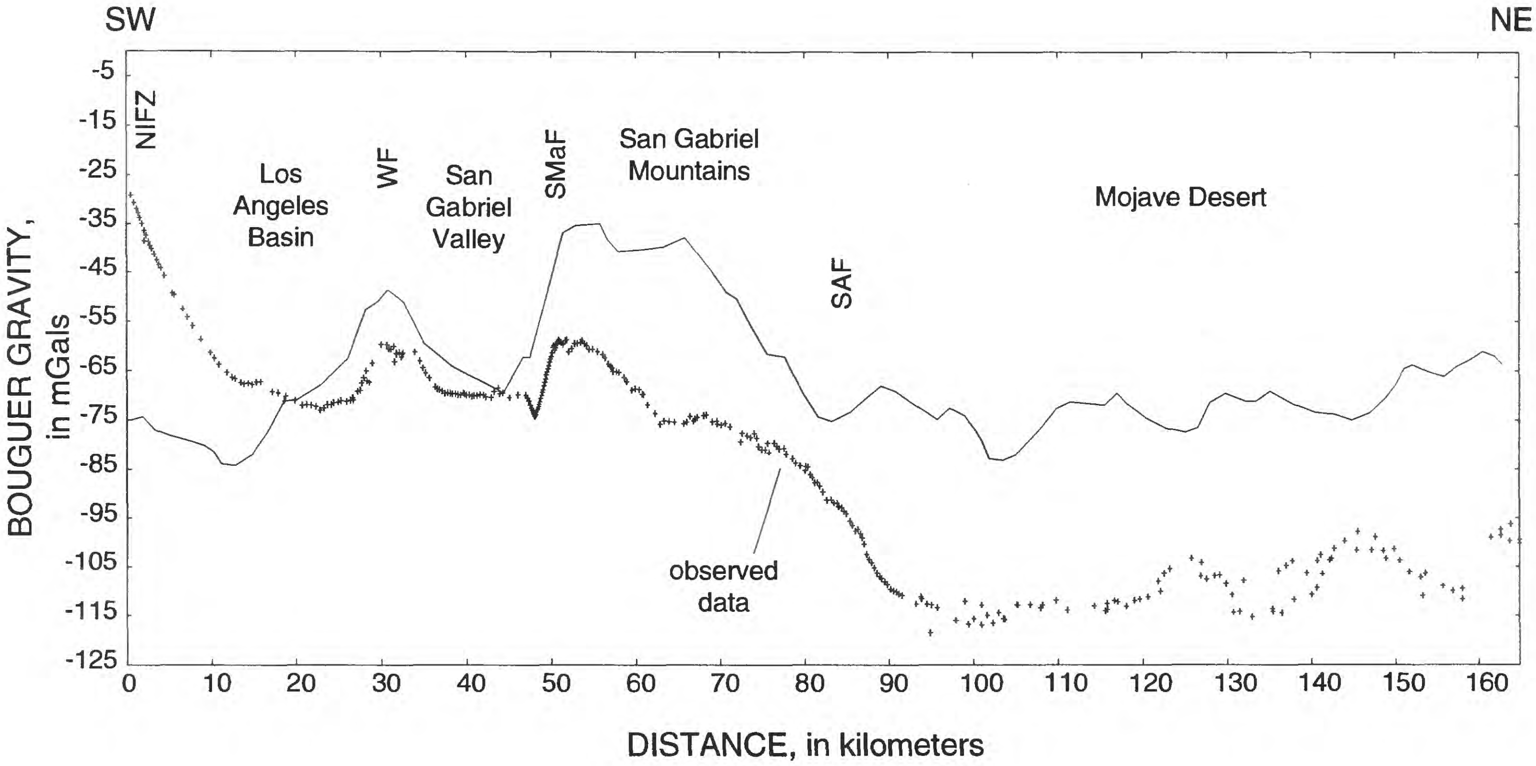

Figure 3d. Calculated gravity curve from Kohler (1999). Her model incorporates depth to Moho, mantle density variations (based on tomography results), and upper crustal density variations based on slow velocity sedimentary and basement rocks from Lutter and others (1999). She assumes a constant density of 2670 kg/m^3 for most of the crust.

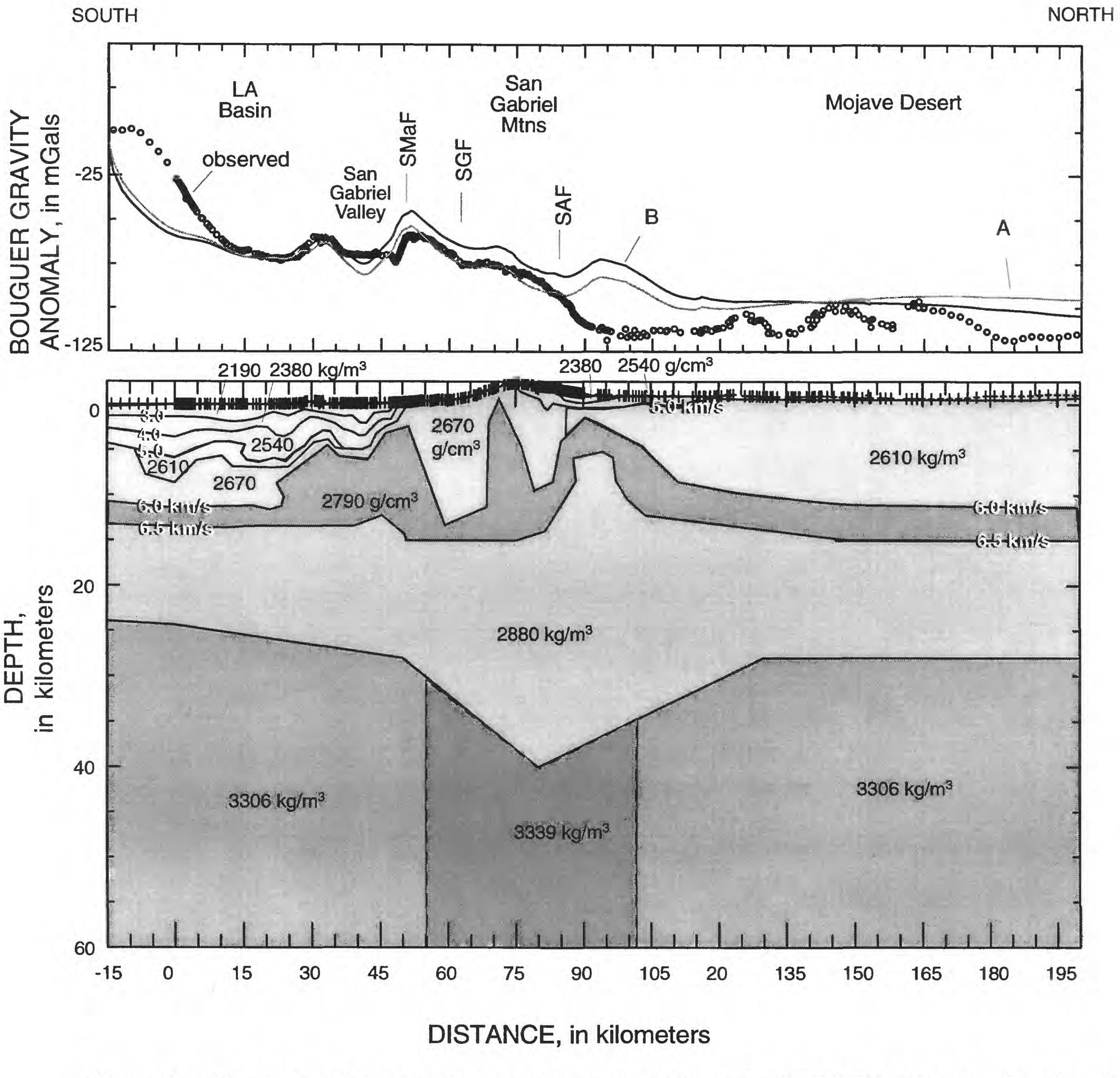

Figure 4a. Gravity model using the velocity structure from the LARSE 1 seismic refraction data (Fuis and others, 1996). Dashed outline shows high-velocity anomaly in mantle, which in this model extends to 200 km. Curve A, calculated without the high-velocity mantle; Curve B, with mantle anomaly.

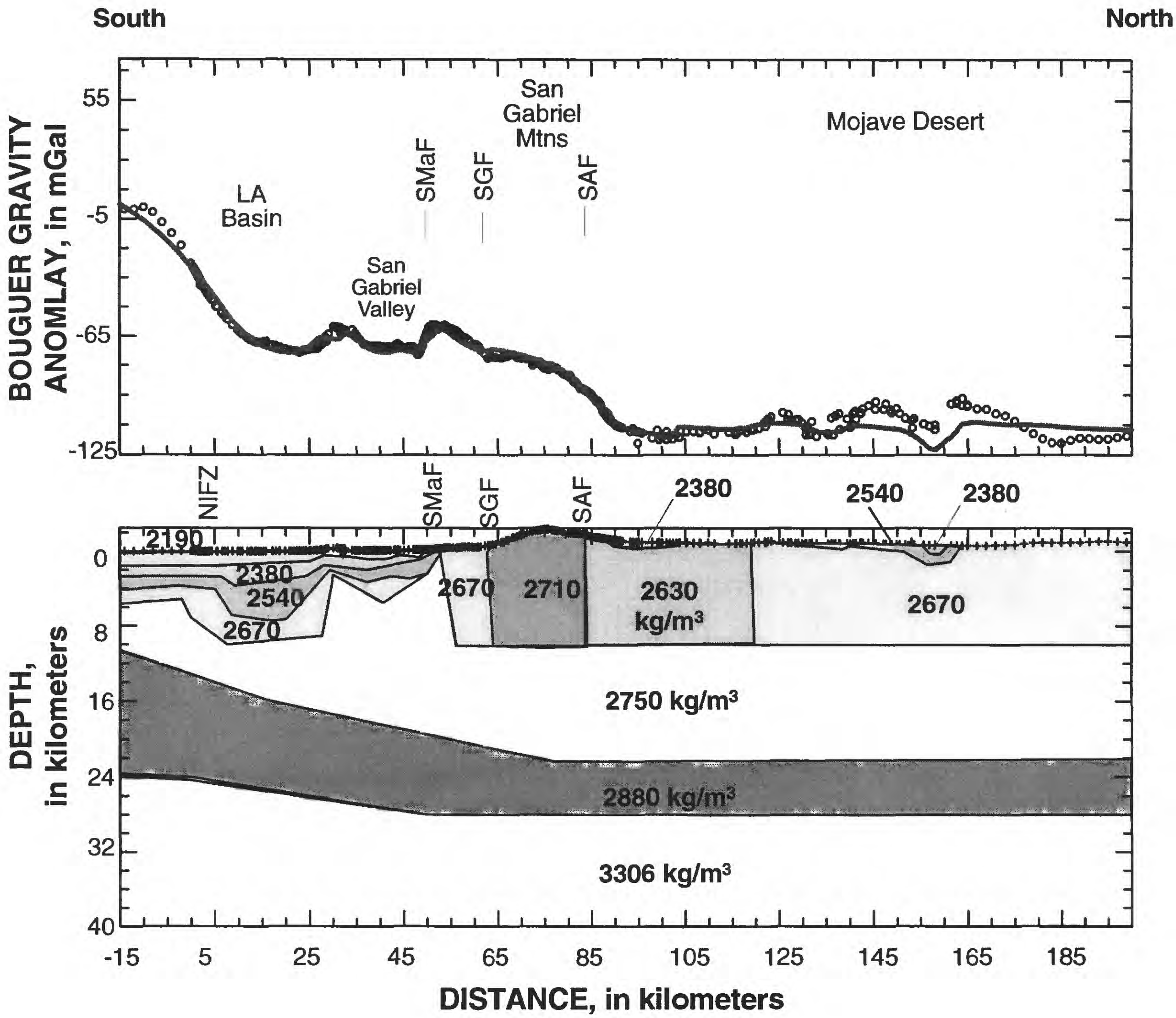

Figure 4b. Gravity model with no crustal root or anomalous mantle. Velocity strucure from Fuis and others (1996) has been modified, especially over the Transverse Ranges and the Mojave Desert. NIFZ, Newport Inglewood fault zone; SAF, San Andreas fault; SGF, San Gabriel fault; SMaF, Sierra Madre fault.

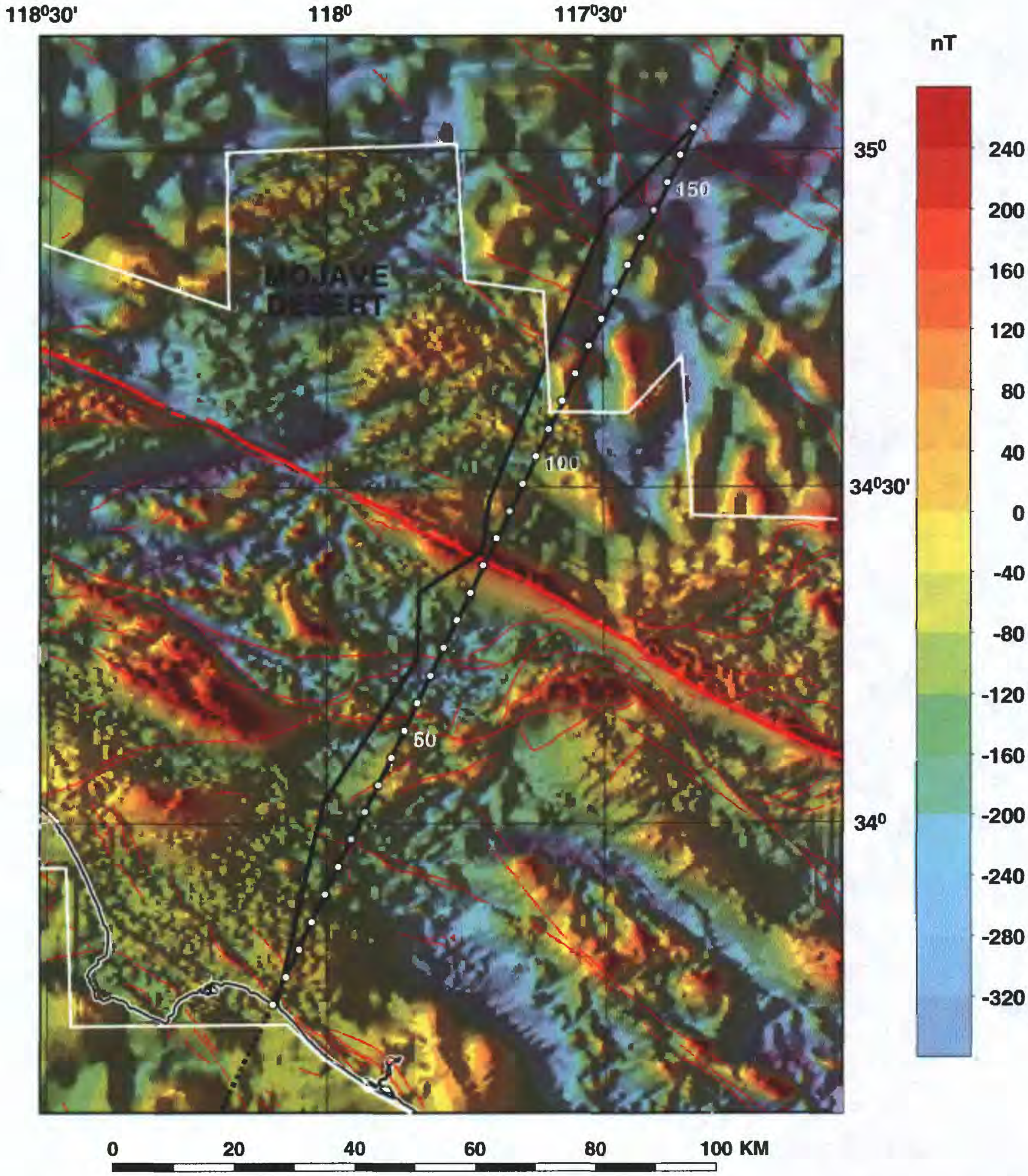

Figure 5. Aeromagnetic map of the LARSE I region. Modeled line is single straight segment. White circles mark 5 km increments along modeled profile. White line shows extent of high-resolution aeromagnetic data over the San Andreas region.

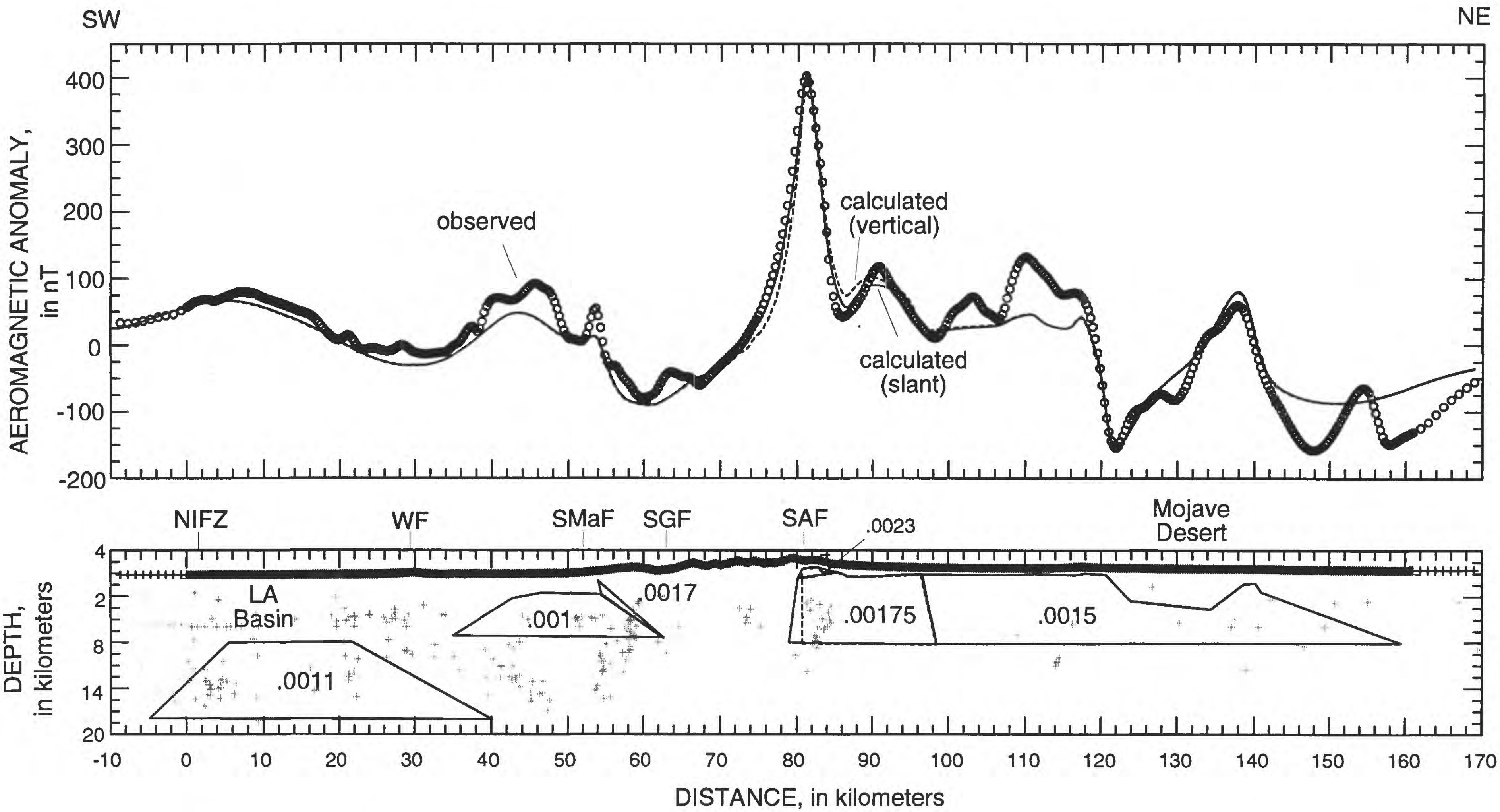

Figure 6a. Model of magnetic data along LARSE 1 transect. Numbers are magnetic susceptibilities in cgs units. No vertical exaggeration. Gray crosses are earthquakes within 10 km projected onto the profile (1981-1994).

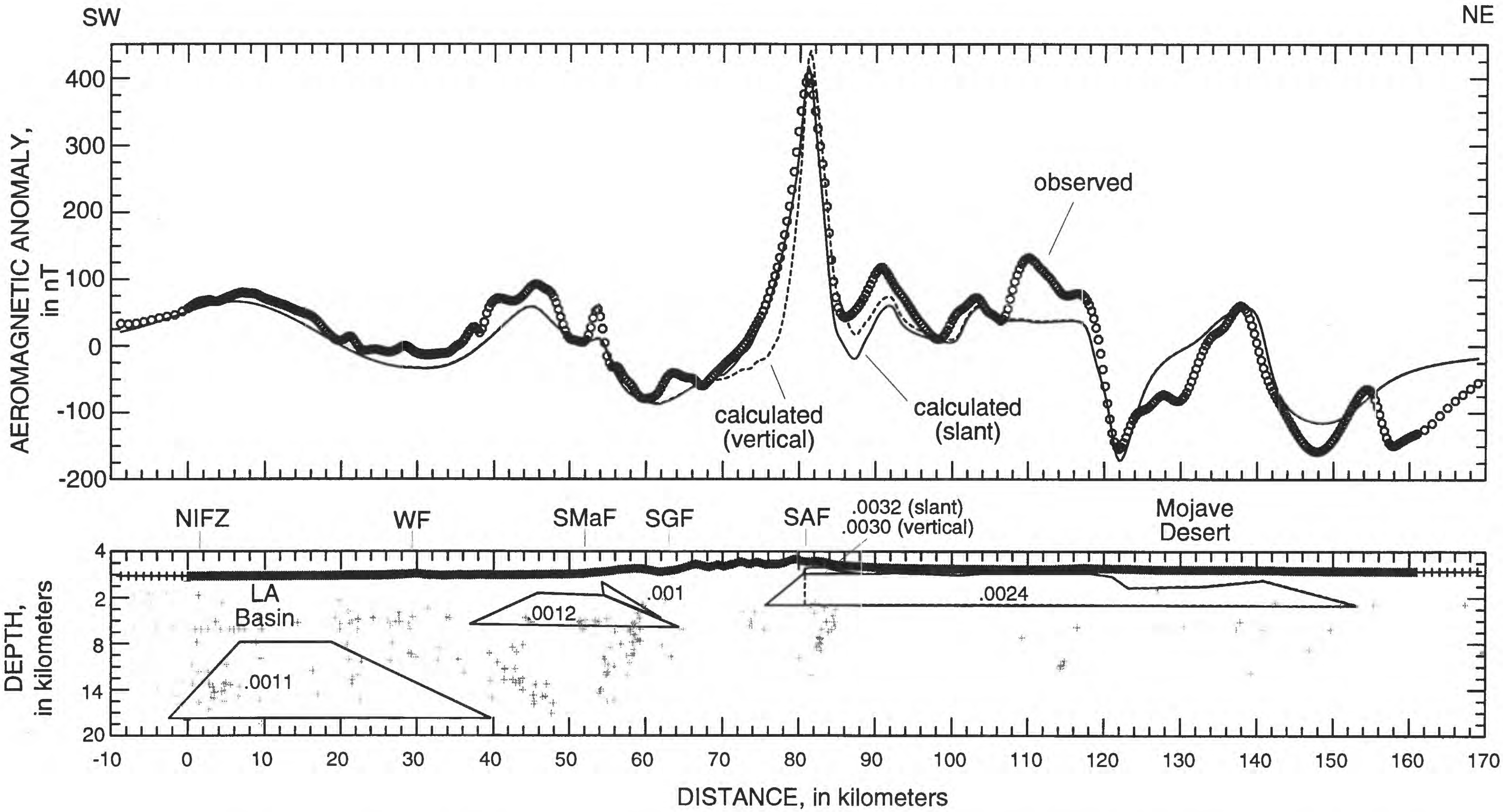

Figure 6b. Model of magnetic data along LARSE 1 transect. Numbers are magnetic susceptibilities in cgs units. No vertical exaggeration. Gray crosses are earthquakes within 10 km projected onto the profile (1981-1994).